LUND UNIVERSITY

Genentech
*A Member of the Roche Group*

# Towards Identifying Pharmacodynamic Blood Biomarkers of MAP3K12 Inhibition

*Master Thesis*

*Elisabeth Jirström*

*August 2017*

**Principal Supervisor**
Cedric Dicko
Department of Pure and Applied Biochemistry
Lund University

**Examiner**
Prof. Leif Bülow
Department of Pure and Applied Biochemistry
Lund University

**Assistant Supervisor**
Felix Yeh
OMNI Biomarker Development
Genentech, Inc.

# Abstract

Amyotrophic lateral sclerosis (ALS) is a neurodegenerative disease characterized by progressive degeneration of upper and lower motor neurons in the brain and spinal cord, for which there is no cure. Activation of the stress-induced c-Jun N-terminal kinase (JNK) signaling pathway, a critical mediator of neuronal apoptosis and axon degeneration, is evident in ALS and is therefore considered a potential target to prevent neurodegeneration. Pharmacological inhibition of an upstream activator of the JNK pathway, the mitogen-activated protein kinase kinase kinase (MAP3K12), has demonstrated neuroprotection *in vitro* as well as suppression of pathway activation *in vivo*. These observations, along with the largely neuronal-specific expression of MAP3K12, makes inhibition of this kinase a promising therapeutic target for ALS. Furthermore, a pharmacodynamic (PD) blood biomarker would be beneficial to help assess efficacy of MAP3K12 inhibition. A crucial step to interpreting the PD effects of MAP3K12 inhibition using blood biomarkers is to acquire evidence of MAP3K12 protein expression in blood, which was the aim of this study. First, we found *Map3k12* transcript levels to be highly reduced in blood from *Map3k12* conditional knockout (cKO) mice, demonstrating that these are excellent negative controls for studying MAP3K12 expression in blood. Next, three antibodies were identified that recognized mouse and human MAP3K12. Utilizing these antibodies, an intracellular flow cytometry method was developed that successfully detected MAP3K12 protein in human peripheral blood mononuclear cells (PBMCs). Collectively, our data provide evidence of MAP3K12 expression in human blood and thus pave the way for identifying PD blood biomarkers of MAP3K12 inhibition.

# Acknowledgements

*This Master thesis was conducted within the Department of OMNI Biomarker Development at Genentech, Inc. in South San Francisco, U.S. during the spring/summer of 2017.*

I would first like to thank my supervisor at Genentech, Felix Yeh, for his immense support, knowledge and enthusiasm throughout my thesis work, and for inspiring and encouraging me to pursue a career in neuroscience.

A special word of thanks goes to Brady Burgess for his extensive support and helpful input. I also wish to thank Martin Larhammar for all his help and encouragement.

My sincere thanks also goes to Heleen Scheerens, Lee Honigberg, Karin Rosen and Allan Gordon with family for setting my degree work in motion, which made my time at Genentech possible.

I thank my colleagues at the Department of OMNI Biomarker Development for their warm welcoming, support both inside and outside the lab and for all the fun times.

I would also like to express my gratitude to my principal supervisor at Lund University, Cedric Dicko, for his committed guidance, availability and positive attitude and my examiner, Leif Bülow, for his support before and throughout the degree project.

Finally, I would like to thank my family and friends for their continuous support and encouragement.

# List of Abbreviations

| | |
|---|---|
| Ab | Antibody |
| ALS | Amyotrophic lateral sclerosis |
| cKO | Conditional knockout |
| JNK | c-Jun N-terminal kinase |
| KO | Knockout |
| MAP3K12 | Mitogen-activated protein kinase kinase kinase 12 |
| PBMC | Peripheral blood mononuclear cell |
| PD | Pharmacodynamic |
| qPCR | Quantitative polymerase chain reaction |
| WT | Wild-type |
| 293 cells | Human embryonic kidney 293 cells |

# Table of Contents

# 1 Introduction

Neurodegeneration is a pathological condition involving the progressive loss of neurons[1]. ALS, also known as Lou Gehrig's disease and motor neuron disease, is a rapidly progressive and invariably fatal neurodegenerative disease[2]. The disease is characterized by loss of motor neurons in the brain and spinal cord resulting in gradual weakness and ultimately paralysis of the innervated voluntary muscles. ALS is a rare disease with a prevalence of approximately 5 patients per 100,000 individuals. The onset of disease usually occurs at a mean age of 55 and death follows typically 3-5 years after diagnosis, mostly from respiratory failure. Approximately 10 % of ALS patients have the familial form of the disease, largely associated with genetic mutations with high penetrance, while about 90% of ALS cases occur sporadically. The cause for the vast majority of ALS cases is unknown, and to date, there is no cure[2,3].

Axon degeneration is a common pathological feature in many neurodegenerative diseases, characterized by the progressive breakdown of axons[4,5]. MAP3K12 has been demonstrated to play an important role in controlling axonal growth, apoptosis during neural development as well as neurodegeneration[6]. In response to neuronal injury, MAP3K12 regulates the mitogen-activated protein kinase (MAPK) cascade, leading to activation of the c-Jun N-terminal kinase (JNK) stress-induced signaling pathway. This results in phosphorylation of the kinase JNK, causing it to translocate to the nucleus, where it in turn phosphorylates the protein c-Jun, leading to the transcription of *JUN* and other genes that mediate axon degeneration and apoptosis[7]. While inhibition of JNK has strong neuroprotective effects *in vitro*, a JNK inhibitor has yet to reach the clinic due to side effects. More specifically, complications would be expected due to JNKs ubiquitous expression and numerous functions outside neurodegeneration, including regulation of cell proliferation[8-11]. An alternative approach to direct inhibition of JNK is to target upstream MAP3K12 that is highly enriched in postmitotic neurons[7], and could thus provide greater temporal and spatial selectivity. In fact, selective MAP3K12 inhibitors have demonstrated neuroprotective activity *in vitro* and suppression of c-Jun phosphorylation in injury models and therefore represent promising candidates for treatment of neurodegenerative diseases, such as ALS[8,9,12].

In this study, we sought to discover a peripheral biomarker to monitor the PD effects of MAP3K12 inhibitors. MAP3K12 is found at the transcript level in blood[13], which makes this a promising matrix for evaluating PD biomarkers of MAP3K12 activity. As MAP3K12 activity regulates transcription of c-Jun regulated genes, potential biomarkers could be measured using quantitative polymerase chain reaction (qPCR) that enable quantification of gene expression and is a suitable technique to use for

clinical applications such as monitoring drug responses[14]. In addition, collection of blood is a less invasive procedure compared to collection of cerebrospinal fluid (CSF) through lumbar puncture. Taken together, development of a blood biomarker would be of great therapeutic importance.

A key step to evaluating the utility of blood-based biomarkers was to determine whether MAP3K12 is expressed at the protein level. To achieve this, we used various techniques including western blot and flow cytometry. Confirmation of MAP3K12 protein expression in blood could pave the way for RNA sequencing (RNAseq) experiments to identify candidate genes that are modulated in response to inhibition of MAP3K12. This would be a first step to discover an expression-based blood biomarker to help predict MAP3K12 pathway inhibition.

# 2 Background

## 2.1 Neuropathological features and genetics of ALS

The primary pathology of ALS is the progressive degeneration of motor neurons in the motor cortex, brain stem and spinal cord (Fig. 1). The etymology of ALS reflects both the loss of spinal motor neurons (lower motor neurons), causing atrophy of target muscles (amyotrophy), and the degeneration of descending corticospinal neurons (upper motor neurons), causing scarring of axons in the lateral tracts of the spinal cord (lateral sclerosis)[2]. Similar to other neurodegenerative disorders the disease starts locally and progressively spreads, causing atrophy and weakness of muscles throughout the body[2,15].

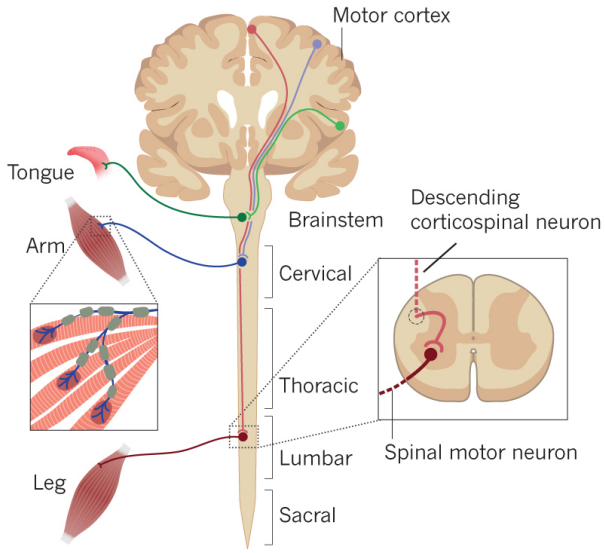


**Figure 1. ALS causes degeneration of motor neurons in the brain and spinal cord.** ALS affects the descending upper motor neurons (originating in motor cortex projecting into the brain stem and spinal cord) and the lower motor neurons (projecting from the lumbar tract into skeletal muscles). Artwork retrieved from "Decoding ALS: from genes to mechanism" on 06/22/17 [doi:10.1038/nature20413].

The onset location and specific early symptoms depend on which motor neurons are first afflicted. The majority of patients have spinal-onset ALS, where motor neurons in the motor cortex and spinal cord are the first to degenerate. This form of the disease is characterized by asymmetric weakness in limbs, where symptoms including muscle atrophy and twitching indicate involvement of lower motor neurons, while hyperreflexia and hypertonia reflect upper motor neuron degeneration. Approximately 20% of patients present bulbar-onset ALS causing degeneration of brain stem motor neurons. These neurons innervate muscles of the mouth and throat and thus give rise to early symptoms such as speech and swallowing difficulties. Patients with spinal-onset ALS have an average survival time of 3-5 years following diagnosis while patients presenting bulbar-onset have an even worse prognosis with an average of 2 years[16].

Sporadic ALS (sALS) is the most common form of the disease and accounts for about 90% of all cases, with the majority having unknown etiology and lacking clear genetic cause. The remaining 10% are cases of familial form of ALS (fALS) that are mainly caused by genetic inheritance[17]. In 1993, fALS causative mutations were found in the gene *SOD1,* encoding the antioxidant enzyme superoxide dismutase 1. Since then, advancements in DNA sequencing technology have led to the discovery of a number of other genes, including *C9orf72*, *TARDBP* and *FUS*, in which mutations cause ALS[16,18]. The rapid progress in genetics of ALS combined with histological discoveries from post-mortem studies of ALS cases have provided insight into the molecular mechanisms and pathways underlying the disease[19].

Glutamate excitotoxicity has been suggested as a major pathogenic mechanism in ALS[20]. Excitotoxicity occurs from excessive stimulation of glutamate receptors that leads to an overload of neuronal calcium influx, which in turn triggers neurodegeneration. Glutamate excitotoxicity has also been implicated in axon degeneration, which is an early pathological feature in ALS[20-22]. Thus, it is of great importance to get a better understanding of how excitotoxicity could initiate pathways mediating neuronal death and axon degeneration.

## 2.2 The role of MAP3K12 in axon degeneration and neuronal apoptosis

MAPKs are a family of evolutionary-conserved serine-threonine protein kinases that are expressed in all eukaryotic cells where they control a diverse set of cellular processes including proliferation, differentiation, stress response and apoptosis[23,24]. Multiple MAPKs exist and are components of a phosphorylation cascade that relay and amplify intracellular signals in response to a variety of extracellular stimuli including cytokines, hormones, neurotransmitters, growth factors and cellular stress[23]. Each cascade consists of at least three kinases, including MAPK and two of its upstream kinases, MAPK kinase (MAP2K) and MAPK kinase kinase (MAP3K). Upon stimulation, MAP3Ks become activated and then phosphorylate and activate MAP2Ks, which in turn phosphorylate MAPKs. This sequential activation of MAPK ultimately leads to activation of target regulatory proteins controlling cellular programs[24].

The JNK stress-induced signaling pathway is one of the major MAPK pathways that have been identified in mammals[23,24]. This pathway takes its name after the JNK group of MAPKs, compromising the three isoforms JNK1, JNK2 and JNK3 (also known as MAPK8, MAPK9 and MAPK10, respectively). The JNK pathway is involved in multiple physiological processes including control of axon degeneration, neuronal apoptosis as well as neuronal homeostasis[23]. MAP3K12 is a

mixed-lineage protein kinase, which is mainly expressed in neurons, and can function as an activator of the JNK pathway[24,25]. MAP3K12 mediated pathway activation and subsequent neurodegeneration is evident in cultured dorsal root ganglion (DRG) neurons from mice in response to nerve growth factor (NGF) deprivation[7]. Moreover, axonal injury causes upregulation of MAP3K12 protein expression in retinal ganglion cells (RGCs) from mice[26].

In response to a variety of neuronal stresses, dual specificity mitogen-activated protein kinase kinase 4 and 7 (MAP2K4 and MAP2K7) become activated by MAP3K12 and in turn activate JNK2 and JNK3[7,11,27] (Fig. 2). Upon activation, phosphorylated JNKs translocate to the nucleus where they phosphorylate the protein c-Jun which in turn upregulates expression of pro-apoptotic genes. Interestingly, MAP3K12 mediated axon degeneration seems to be c-Jun independent and caused by phosphorylation of distinct JNK targets[7].

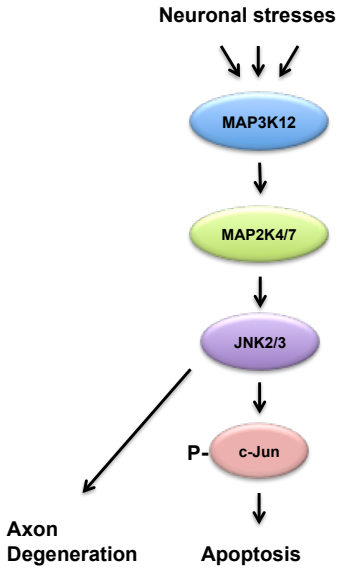


**Figure 2. A model for apoptosis and axon degeneration through MAP3K12 mediated activation of the JNK stress-induced pathway.** MAP3K12 is activated in response to neuronal stress leading to the sequential activation of MAP2K4/7 and JNK 2 and 3. Next, phosphorylated JNKs are transported to the nucleus where they phosphorylate c-Jun, which in turn leads to transcription of genes mediating apoptosis. Downstream JNK-activated targets mediate axon degeneration through a c-Jun independent process.

## 2.3 The therapeutic potential of inhibiting the MAP3K12/JNK pathway in ALS

ALS is a disease with high-unmet need and as of yet, no good therapeutic options exist. The standard of care includes the drug Riluzole, which extends survival by about two months over 18 months of treatment. Unfortunately, patients gain no improvements in overall function or muscular strength and the treatment comes with many side effects, including fatigue and nausea[28]. Recently, the U.S Food and Drug Administration (FDA) approved a new drug, Radicava. This drug slowed the functional decline in a trial of patients with early-stage ALS, but the effects on survival have yet to be evaluated[29]. In order to develop novel disease modifying treatments that can change the course of

this disease and improve patient survival, it is of great importance to advance the understanding of the molecular mechanisms mediating pathogenesis of ALS.

Increased levels of phosphorylated c-Jun, a marker for JNK pathway activation, have been found in the spinal cord of ALS patients and ALS mouse models[30-32]. Reductions in apoptosis, axon degeneration and phosphorylated c-Jun levels have been observed in cultured primary DRG neurons from *Map3k12* knockout (KO) mice embryos compared to WT controls, following cellular stress induced through NGF withdrawal[7]. Interestingly, global deletion of *Map3k12* in adult mice strongly protects RGCs from apoptosis following axonal injury via optic nerve crush[26]. Furthermore, *Map3k12* cKO adult mice have a reduction in neurodegeneration following excitotoxicity–induced cell death *in vivo*[33]. Collectively, these studies suggest that MAP3K12 regulates the JNK stress-induced pathway following NGF withdrawal, axonal injury and excitotoxicity and that loss of MAP3K12 is neuroprotective. These findings, in conjunction with the implicated glutamate excitotoxicity pathogenic process in ALS[21], strongly suggests that inhibition of MAP3K12/JNK pathway could be a potential therapeutic target for treatment of ALS.

The role of the JNK stress-induced pathway signaling in neurodegenerative diseases, such as ALS, has resulted in significant efforts towards developing inhibitors of this pathway[8]. Inhibition of JNK protects cortical neurons and RGCs against excitotoxicity-induced death *in vitro* as well as *in vivo* following brain injury[34,35]. However, the ubiquitous expression of JNKs along with their roles in both pathological and physiological functions implies that potential side effects could arise from use of JNK inhibitors. Consequently, there has been no approval of JNK inhibitors for use in humans[8-11]. Thus, efforts have been made to find an alternative approach to direct inhibition of JNK. The selective expression of MAP3K12 in the brain in conjunction with its role as an upstream activator of the JNK pathway makes it a promising therapeutic candidate. Recently, novel selective MAP3K12 inhibitors have been developed through high-throughput screening against the catalytic kinase domain of MAP3K12. These small-molecule inhibitors have strong neuroprotection *in vitro* in rat primary DRG neurons and embryonic stem cell (ESC) derived RGCs[8,36]. Furthermore, inhibition of MAP3K12 *in vivo* suppressed c-Jun phosphorylation in both a mouse optic nerve crush model of axonal injury and in a Parkinson's disease mouse model of neurodegeneration[8]. Taken together, these findings suggest a potential for MAP3K12 inhibitors as disease modifying therapeutics for neurodegenerative diseases.

## 2.4 Using expression-based peripheral blood biomarkers to help predict MAP3K12 inhibition

Biomarkers are important tools in drug discovery and development with a wide range of applications. These include evaluation of drug safety, efficacy, changes in biological pathways and target engagement[37]. The need for PD biomarkers in ALS drug development is of great importance since demonstration of drug efficacy and target engagement in the nervous system could help guide dose selection, contribute to reducing the length and increasing the chances of successful clinical trials[38,39].

Here, we sought to identify a gene expression-based biomarker to measure the PD effects of MAP3K12 inhibitors. This has advantages over assaying for the phosphorylation state of the MAPKs due to the transient nature of these events[40]. Furthermore, MAP3K12 mediated transcriptional changes of c-Jun regulated genes could be detected using RNAseq and easily measured using qPCR, and are thus promising biomarkers of MAP3K12.

MAP3K12 is expressed at the RNA level in human peripheral blood[13], which makes blood a promising source for measuring PD biomarkers of MAP3K12. However, interpretation of the PD effects of MAP3K12 inhibition requires evidence of protein expression, which has not, to the best of our knowledge, been identified in blood. Therefore, the main focus of this study was to investigate whether MAP3K12 protein is expressed in human peripheral blood.

# 3 Material and Methods

## 3.1 Mouse models

*Map3k12* cKO mice were generated by crossing mice having exons 2-5 (DNA encoding kinase domain of MAP3K12) flanked by loxP sites (*Map3k12*$^{loxp/loxp}$)[7] with mice carrying a cytomegalovirus (CMV) early enhancer/chicken $\beta$-actin (CAG) promotor driven Cre recombinase-estrogen receptor transgene (Cre-ERT)[41] obtained from The Jackson Laboratory. To induce *Map3k12* recombination and excision of *Map3k12* in brain and peripheral tissue, both *Map3k12*$^{loxp/loxp}$/Cre-ERT$^{pos}$ mice (referred to as *Map3k12*$^{loxp}$;Cre$^{pos}$) and their littermate controls (*Map3k12*$^{loxp}$;Cre$^{neg}$) were fed tamoxifen for 3 weeks, put back on a regular diet and used in experiments after approximately one year.

All animal procedures were reviewed and approved by the Institutional Animal Care and Use Committee at Genentech and are in accordance with the NIH's Guide for the Care and Use of Laboratory Animals.

## 3.2 qPCR

Total RNA was isolated from whole blood and brain tissue (collected from *Map3k12*$^{loxp}$;Cre$^{pos}$ and *Map3k12*$^{loxp}$;Cre$^{neg}$ mice) using the RiboPure™ Blood RNA Purification Kit (Invitrogen) and the RNeasy Mini Kit (Qiagen), respectively. RNA purity and concentrations were measured using a NanoDrop Spectrophotometer and equal amounts of cDNA were synthesized using the High-Capacity cDNA Reverse Transcription Kit (Thermo Fischer Scientific). qPCR analysis was performed using TaqMan Fast Advanced Master Mix (Applied Biosystems) and pre-designed TaqMan Gene Expression Assays (Applied Biosystems) on a ViiA 7 Real-Time PCR system (Applied Biosystems). Assay ID for each pair of *Map3k12* TaqMan primers (labeled with FAM dye) were as follows: Mm01303169_m1 (referred to as probe 1), Mm01296205_m1 (referred to as probe 2) and Mm01296200_g1 (referred to as probe 3). *Gapdh* was used as endogenous control and detected using a VIC-labeled set of TaqMan primers (Assay ID: NM_008084.2, Applied Biosystems). *Gapdh* and *Map3k12* primers were multiplexed. The qPCR data was analyzed using $\Delta$Ct (Ct = cycles to threshold) values that demonstrate the difference of gene expression between *Map3k12* and *Gapdh* as well as $\Delta\Delta$Ct values that demonstrate difference between $\Delta$Ct for *Map3k12*$^{loxp}$;Cre$^{pos}$ mice and *Map3k12*$^{loxp}$;Cre$^{neg}$ mice . The $2^{-\Delta\Delta Ct}$ – method was used to calculate the relative expression of *Map3k12* between *Map3k12*$^{loxp}$;Cre$^{pos}$ mice and *Map3k12*$^{loxp}$;Cre$^{neg}$ mice.

Prism7 (Graphpad) was used for statistical analysis with p-values determined by the *Two stage set-up method of Benjami Krieger and Yekutieli.*

## 3.3 Cell cultures

Stable MAP3K12 expressing cells were generated as previously described[42]. Briefly, human *MAP3K12* was cloned into a pTRE2hyg vector and subsequently transfected into 293 Tet-ON cells. Selected cells were grown to 70-80 % confluence and then subjected to 3 uM doxycycline (DOX) to induce MAP3K12 expression. 24 hours later, cells were either lysed for western blot analysis or trypsinized for flow cytometry analysis.

## 3.4 Western blotting

Brain tissue (~500 ug/mouse) was harvested from *Map3k12*$^{loxp}$;Cre$^{pos}$ and M*ap3k12*$^{loxp}$;Cre$^{neg}$ mice and lysed in radioimmunoprecipitation assay (RIPA) buffer (50 mM Tris, 150 mM NaCl, 2 mM EDTA, 10% NP-40, 0.1% SDS, pH 7.4) containing protease and phosphatase inhibitor cocktails (Roche) and benzonase nuclease (Sigma Aldrich) using a tissue homogenizer (Bertin) with 1.4 mm ceramic beads (Qiagen). Brain lysate was centrifuged at 20,000 x g at 4℃ for 15 min for collection of soluble proteins in supernatant. 293 cell cultures were lysed in 1 mL of RIPA buffer for 15 min at 4℃ followed by centrifugation at 20,000 x g at 4℃ for 15 min for collection of soluble protein. Protein amounts were determined using Pierce™ BCA protein assay (Thermo Fischer Scientific) and iMark™ Microplate Absorbance Reader (Bio-rad).

Lysate was resuspended in NuPAGE LDS Sample Buffer (Invitrogen) containing NuPAGE Sample Reducing Agent (Invitrogen), incubated at 70℃ for 10 min and loaded on 4-12% Bis-Tris gels (Invitrogen). Gels were run in NuPAGE MOPS SDS Running Buffer (Invitrogen) at 200V using Powerpac™ power supply (Bio-rad).

Proteins were transferred onto 0.2 μm nitrocellulose membranes using iBlot® 7-Minute Blotting System (Invitrogen). To block unspecific binding, blotted membranes were incubated with 5% skim milk (Bio-rad) in TBS-Tween (50 mM Tris, 150 mM NaCl 0.1% Tween 20, pH 7.5) for 1 h at room temperature (RT). For immunodetection, membranes were incubated for 24 h at 4°C with primary antibodies (Table S1), washed 3x5 min with TBS-Tween and incubated for 2 h at RT with secondary HRP-conjugated antibodies (Table S1). Blots were developed with enhanced chemiluminescence (SuperSignal West Dura or SuperSignal West Dura Femto) detection system (Thermo Fisher Scientific) and imaged using ImageQuant LAS 4000 (GE Healthcare).

## 3.5 Isolation of human PBMCs

Human PBMCs were isolated from K2-EDTA treated peripheral blood of healthy donors by standard Ficoll-Paque Plus density gradient centrifugation (GE Healthcare) using phosphate-buffered saline (PBS) as salt balance solution. PBS was added to fresh blood at a 1:3 ratio, mixed and then layered onto Ficoll-Paque media at a 2:1 ratio and centrifuged at 800 x g for 20 min at RT (brake off). The layer of mononuclear cells was isolated using a sterile pipette. After washing with PBS, PBMCs were collected by centrifugation at 1500 rpm for 5 min at RT (brake on) and used in flow cytometry analysis. Cell viability was determined by trypan blue dye exclusion using the Countess Automated Cell Counter (Invitrogen).

## 3.6 Flow cytometry analysis

For flow cytometry analysis of 293 cells, adherent cells were grown to 70-80 % confluence and then harvested and dissociated using Trypsin-EDTA 0.25% (Gibco) at 37℃ for 5 min.

Fixation and permeabilization of 293 cells and isolated PBMCs were performed as previously described[43]. 293 cell suspensions in staining solution (1% Bovine serum albumin in PBS) were incubated for 10 min at RT with Human BD Fc Block (BD biosciences) prior to immunostaining. Cells were stained with primary antibodies or isotype control (Table S1) for 1 h at RT, washed twice with staining solution and subsequently incubated with a secondary antibody coupled to a fluorescent dye (Table S1) for 30 min at RT. Cells were washed twice and then resuspended in staining media for flow cytometry analysis. Samples were acquired with a BD LSR Fortessa flow cytometer (BD biosciences) and 20,000-30,000 events were analyzed. Fluorescence was measured using Alexa Fluor 647 detection channel (laser line 647) and a FITC channel (laser line 488) was included as a control. Primary gates were set based on forward scatter (FSC) and side scatter (SSC) to exclude cell debris, dead cells and cell doublets. Positively stained cells were gated in accordance to cells stained with isotype controls. FlowJo software (Tree Star) was used for data analysis.

# 4 Results

## 4.1 *Map3k12* transcript is efficiently reduced in whole blood from *Map3k12* cKO mice

As previously described, *Map3k12* cKO mouse models are useful for studying injury/stress-induced neurodegeneration. Here, we sought to investigate whether they can also be used for studying MAP3K12 mediated changes in gene and protein expression in blood. Additionally, an *in vivo* model could be useful to better understand the effects of inhibiting MAP3K12. Before analyzing MAP3K12 protein expression in blood, we needed to assess whether cKO of *Map3k12* results in an adequate loss of the transcript in blood.

Here, we used *Map3k12* cKO mice generated through Cre-lox recombination as previously described[7,41]. This KO technique enables inducible gene deletion at a designated time window, hence circumventing the embryonic lethality that can occur in germline *Map3k12* KO mice[33]. A previous study confirmed that this method results in significant reduction in MAP3K12, on both gene and protein level in brain[33], but the effects in blood have not been previously assessed. Since Cre-ERT is expressed throughout the body[41], recombination should lead to reduced expression of MAP3K12 not only in nervous tissue, but also in peripheral blood. However, as opposed to neurons that enter a post-mitotic state early during development, hematopoietic stem cells are multipotent and can renew in the bone marrow throughout life[44]. Consequently, substantial cKO of *Map3k12* is more difficult to achieve in blood than in brain.

To investigate whether *Map3k12* had been effectively reduced at the mRNA level in blood, qPCR analysis was performed using three different probes specific for different sequences of *Map3k12* (Fig. 3A). Gene expression quantification using probe 1 (Fig. 3, B and E) demonstrated a significant increase in ΔCt values in blood from *Map3k12$^{loxp}$;*Cre$^{pos}$ mice compared to *Map3k12$^{loxp}$*;Cre$^{neg}$ mice and the relative gene expression was quantified to be 30%. As expected, ΔCt values and relative gene expression were reduced in *Map3k12* levels in brain from *Map3k12$^{loxp}$;*Cre$^{pos}$ (~ 30% relative gene expression). Similarly, there was a significant increase in ΔCt values in blood from *Map3k12$^{loxp}$;*Cre$^{pos}$ mice compared to *Map3k12$^{loxp}$*;Cre$^{neg}$ mice and the relative expression of *Map3k12* measured to approximately 15% using probe 2 (Fig. 3, C and F) and 30% using probe 3 (Fig. 3, D and G). An approximate 30 % reduction of *Map3k12* transcript was observed in brain tissue of the cKO mice. Quantification of *Map3k12* in blood from one of the *Map3k12$^{loxp}$;*Cre$^{pos}$ mice resulted in lower ΔCt values compared to the other mice, across all three experiments (Fig. 3B-D). In

contrast, ΔCt values in brain were similar between all mice, suggesting that the variability in blood emerged from issues with sample collection and processing.

Collectively, these data demonstrate a considerable reduction of *Map3k12* in blood from *Map3k12*$^{loxp}$;Cre$^{pos}$ mice compared to *Map3k12*$^{loxp}$;Cre$^{neg}$ mice. *Map3k12* expression was significantly reduced in brain tissue from *Map3k12*$^{loxp}$;Cre$^{pos}$ mice compared to *Map3k12*$^{loxp}$;Cre$^{neg}$ mice, which correlates well with the observations made in a previous study[33]. Interestingly, the reduction observed with both upstream and downstream probes indicates that deletion of the exons encoding the kinase domain of MAP3K12, leads to loss of the entire transcript in both blood and brain tissue. Moreover, these data demonstrate that three weeks of tamoxifen treatment is adequate to achieve long-lasting reduction of *Map3k12* transcript in blood allowing us to assess changes, on both gene and protein level, mediated by MAP3K12.

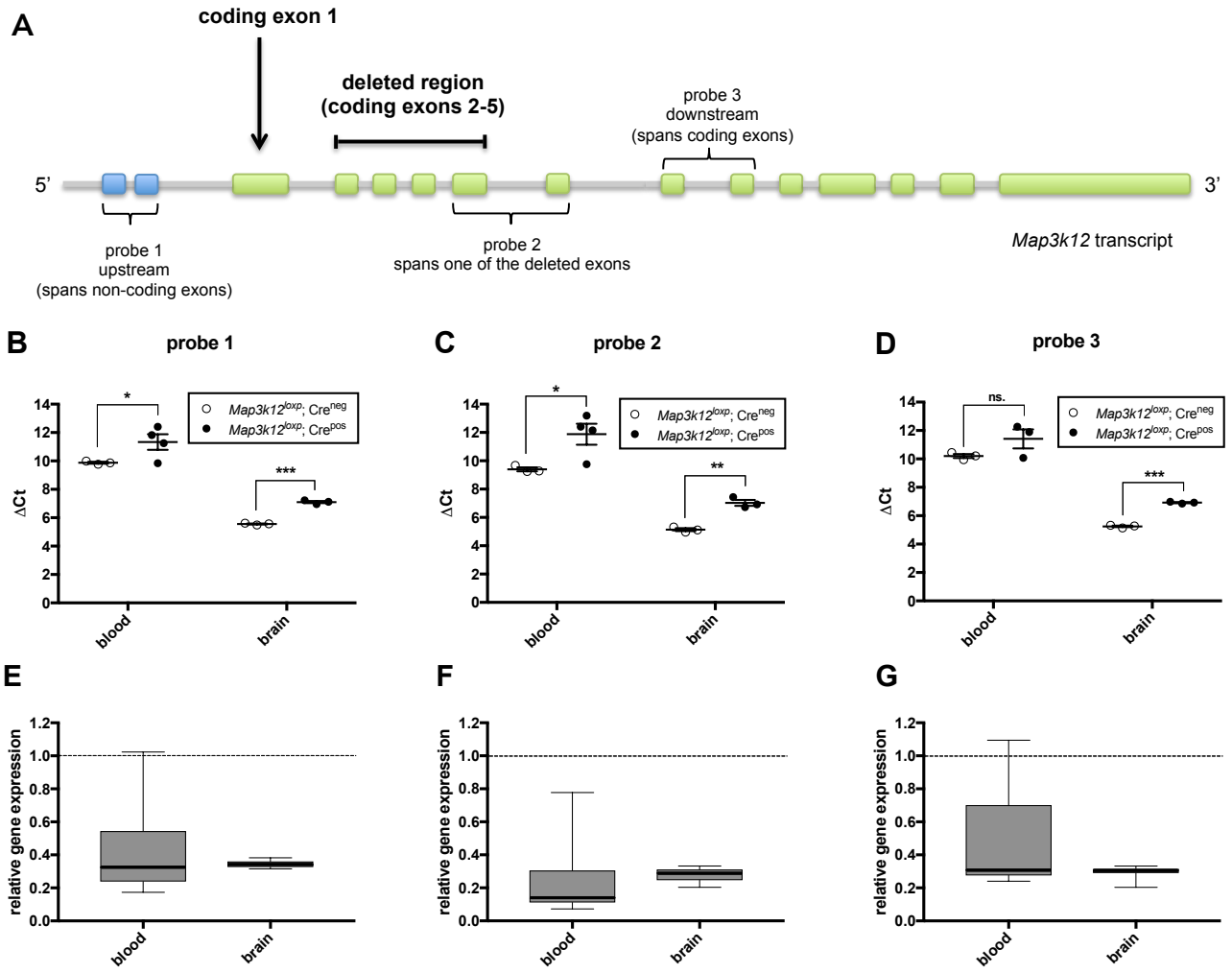


**Figure 3. qPCR analysis of *Map3k12* expression in whole blood and brain tissue from *Map3k12*$^{loxp}$;Cre$^{pos}$ mice relative to *Map3k12*$^{loxp}$;Cre$^{neg}$ mice.** (A) Gene expression analysis was performed using three *Map3k12* specific TaqMan probes targeting different sequences of the gene (positions marked on the resulting Map3k12 transcript). Probe 1 spans two non-coding exons upstream of the deleted region, probe 2 spans two coding exons, one of them within the deleted region and probe 3 spans two coding exons downstream of the deleted region. (B and E) Gene expression quantification using probe 1; (C and F) using probe 2; (D and G) using probe 3. (B-D) Expression of *Map3k12* is presented as ΔCt (normalized to *Gapdh*). Error bars represent +/- SEM for $n \geq 3$. Not significant (ns). $p > 0.1$; * $p < 0.1$; ** $p < 0.01$; *** $p < 0.001$. (E-G) Boxplot representation displays median value (bold line) of relative gene expression ($2^{-\Delta\Delta Ct}$) of *Map3k12* between *Map3k12*$^{loxp}$;Cre$^{pos}$ mice and *Map3k12*$^{loxp}$;Cre$^{neg}$ mice (dashed line). Whiskers represent min and max values for $n \geq 3$.

## 4.2 Three antibodies recognize MAP3K12 by western blot

To investigate whether MAP3K12 is expressed at the protein level in blood, the first step was to identify specific and sensitive anti-MAP3K12 antibodies. More specifically, we sought to find antibodies recognizing both human and mouse MAP3K12 to study the protein in a variety of immunostaining applications including western blot, flow cytometry and immunohistochemistry. For this purpose, seven anti-MAP3K12 antibodies (Table S1, Ab 1-7) were screened by western blot. Out of these seven antibodies, immunoblotting with three demonstrated appreciable levels of MAP3K12 in brain tissue from *Map3k12*$^{loxp}$;Cre$^{neg}$ mice and as anticipated, the protein levels in brain tissue from the *Map3k12*$^{loxp}$;Cre$^{pos}$ mice were highly reduced, mirroring the mRNA data (Fig. 4A). Utilizing a 293 stable cell line where MAP3K12 expression was under the control of DOX, the same three sets of antibodies were also able to detect human MAP3K12. Notably, faint bands corresponding to MAP3K12 were observed for the non-induced 293 cells as well, and this likely is due to basal activity of the promoter causing leaky expression of MAP3K12 (Fig. 4B). The remaining antibodies were unable to recognize both mouse and human MAP3K12, which was concluded based on the lack of bands at the appropriate molecular weight (Fig. 4, A and B). Although bands at the molecular weight of MAP3K12 were observed for 293 cells using Ab 4, these were concluded non-specific given the absence of any noticeable differences between the induced and non-induced lanes.

To summarize, the antibody screen resulted in three antibodies that successfully recognize both mouse and human MAP3K12. Interestingly, each of these antibodies recognize different regions of MAP3K12, where Ab 1 recognizes the C-terminus, Ab 2 the N-terminus and Ab 3 recognizes a sequence within the center region of MAP3K12. As depicted by the intensity of bands, the sensitivity of these three antibodies differs. A more sensitive chemiluminescence substrate was required for detection of MAP3K12 using the C-terminus specific antibody (Ab 1) than for the two other antibodies, suggesting it is less sensitive. Moreover, the center-specific antibody (Ab 3) yielded the strongest bands with a 10 s exposure, compared to a 30 s exposure that was used for Ab 1 and Ab 2. Evidently, Ab 3 outperformed the other two MAP3K12 antibodies, and was concluded to be the most promising candidate for further protein analysis.

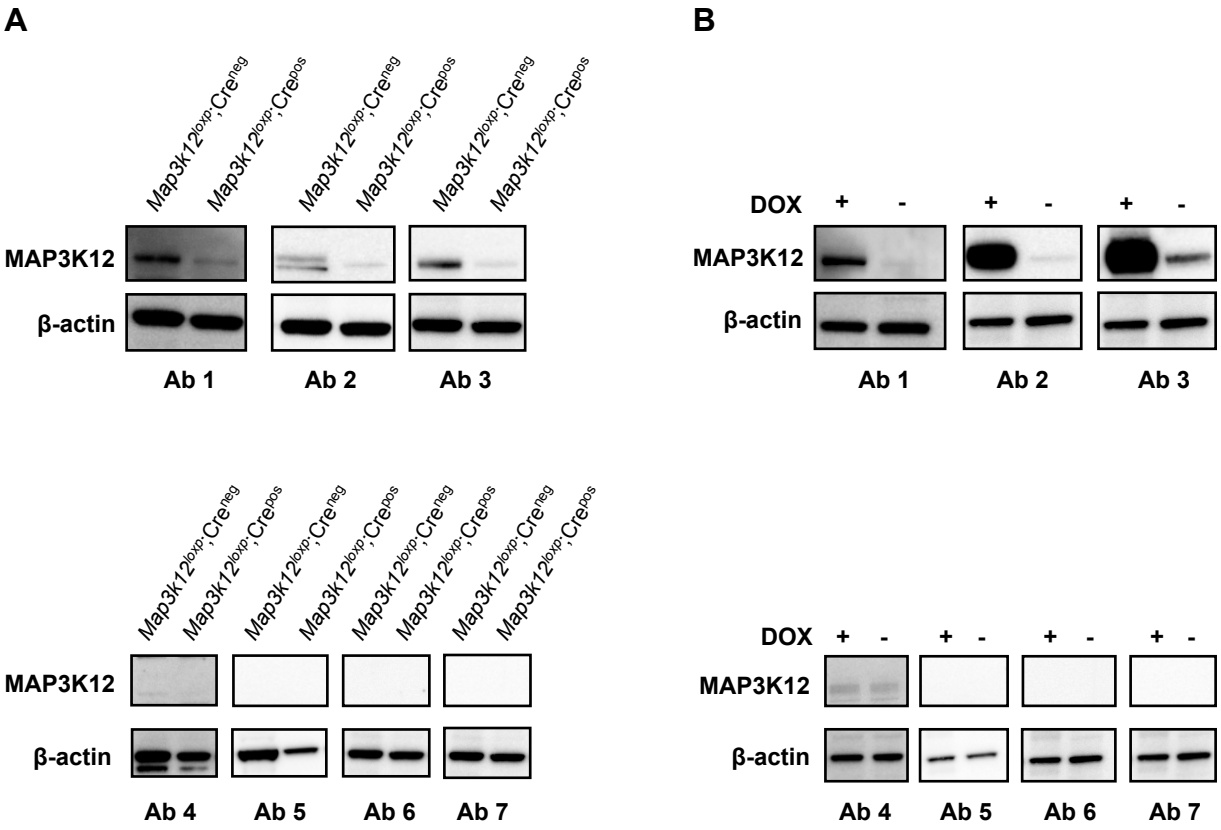


**Figure 4. Western Blot analysis of seven different anti-MAP3K12 Abs (Ab 1-7).** (A) MAP3K12 immunoreactivity in brain tissue lysates from *Map3k12*$^{loxp}$;Cre$^{neg}$ mice and *MAP3K12*$^{loxp}$;Cre$^{pos}$ mice. $\beta$-actin was used as internal loading control. (B) MAP3K12 reactivity in lysates from a MAP3K12 293 stable cell line $\pm$ DOX to control expression of MAP3K12. $\beta$-actin was used as internal loading control.

## 4.3 Evidence of MAP3K12 protein expression in human PBMCs

The antibody screen resulted in three antibodies that recognize MAP3K12 by western blot, and we next asked whether they could be used for protein analysis by flow cytometry. This technique is useful for studying protein expression and has the capability to measure single cell events. An important advantage of flow cytometry over biochemical applications such as western blot is the possibility to analyze samples with complex cell populations, such as human PBMCs, that are composed of a heterogeneous population of immune cell types[43]. Thus, it is a promising method to detect intracellular expression of MAP3K12 in peripheral blood and could provide information about which populations expresses it.

Utilizing the three antibody candidates from the western blot screen, we developed an intracellular flow cytometry method to measure human MAP3K12. This was achieved through fixation and permeabilization of 293 stable cell line where expression of MAP3K12 was inducible in the presence of DOX. The cells were then stained with Ab 1, 2 and 3 followed by an Alexa-647 labeled secondary antibody (Table S1) and analyzed by flow cytometry. To discriminate MAP3K12 positive cells from negative cells, an IgG isotype control was used and the resulting gating scheme is presented in (Fig. S1, A and B).

In general, the flow cytometry results mirrored the observations from our western blot experiments. A very small amount of MAP3K12 positively stained cells were detected for the non-induced 293 cells with Ab 1 (Fig. 5A). In contrast, a large number of non-induced 293 cells stained positive with Ab 2 and Ab 3 (Fig. 5, B and C), but this was concluded to be due to leaky expression of MAP3K12, given that similar observations were made with these two antibodies in western blot. Importantly, noticeable shifts in fluorescence intensity between negative and positive DOX-induced cells were observed with all three antibodies with the vast majority of cells staining positive (Fig. 5, D-F). More specifically, the MAP3K12 center-specific antibody (Ab 3) displayed the greatest shift in intensity of DOX-induced 293 cells, which agrees with the previous observations made by western blot. Collectively, these results demonstrate that all three antibodies are suitable for intracellular flow cytometry analysis of MAP3K12, with Ab 3 demonstrating the greatest sensitivity for human MAP3K12.

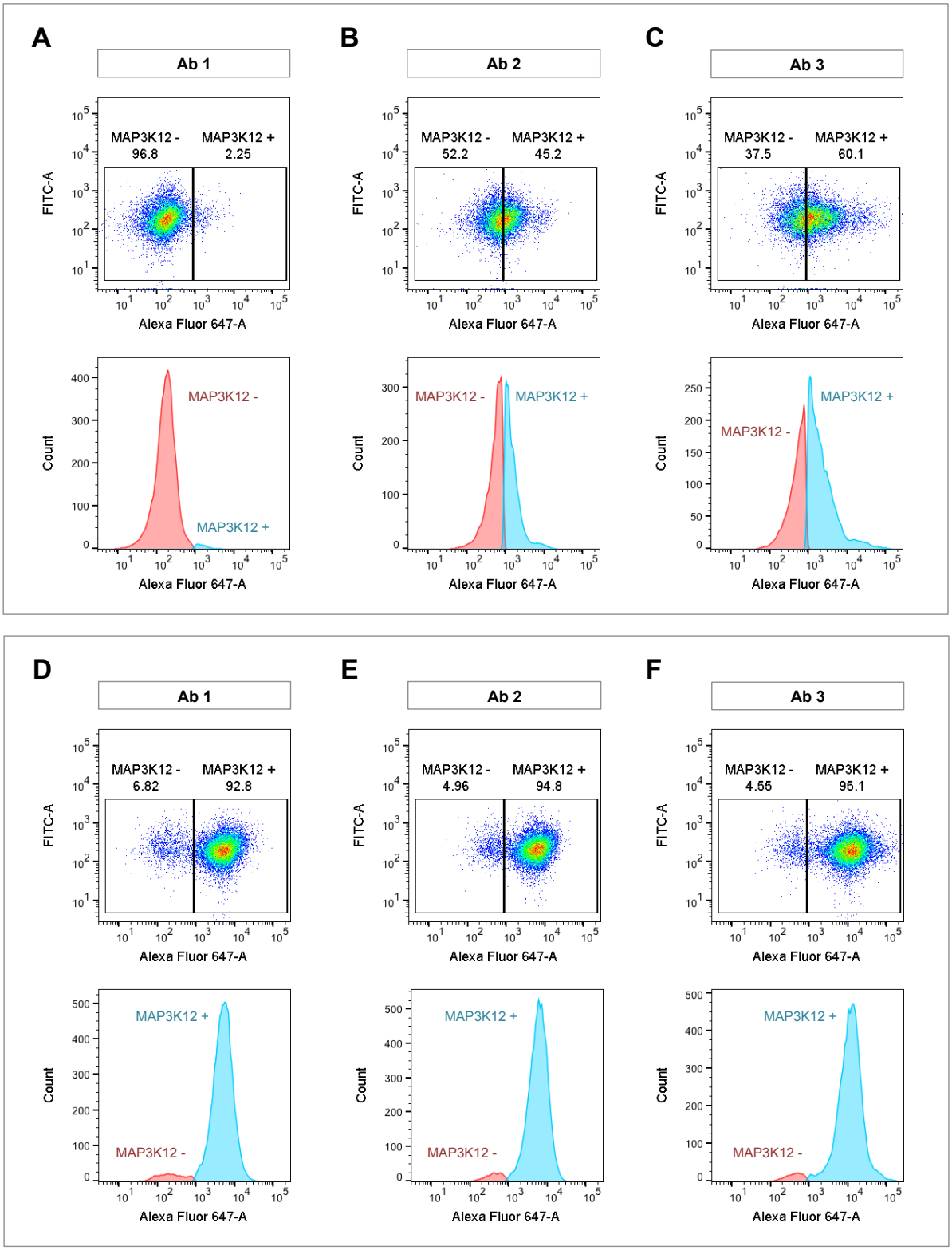


**Figure 5. Flow cytometry analysis of MAP3K12 expression in 293 cells ± DOX-induced MAP3K12 expression following intracellular staining using Ab 1, Ab 2 and Ab 3.** Representative dot plots depict the fluorescence intensity (-A in axis label refers to fluorescence area) and percentages of MAP3K12 positive (+) cells and MAP3K12 negative cells (-). Representative histograms depict fluorescence intensity (x-axis) and number of cells (y-axis). (A-C) Analysis of non-induced 293 cells. (D-F) Analysis of DOX-induced 293 cells.

With a successfully developed intracellular flow method, we could next investigate MAP3K12 protein expression in human peripheral blood. Human PBMCs were isolated from two healthy donors for subsequent flow cytometry analysis in accordance to the previously described flow cytometry method. The resulting gating scheme is presented in (Fig. S1, C and D).

A slight shift in fluorescence intensity was observed for less than 15% of the PBMCs stained with the C-terminus specific antibody (Ab 1), suggesting minimal expression of MAP3K12 in these cells (Fig. 6A). Although, the general absence of MAP3K12 positive cells could be due to the antibody not having the sensitivity required to detect the protein in PBMCs, given that this was the least sensitive antibody in previous western blot and flow cytometry analyses. Interestingly, a larger percentage of PBMCs stained positive with the N-terminus antibody (Ab 2) (Fig. 6B). This data is suggestive for possible expression of MAP3K12 protein in human blood, and remarkably, this kinase seems to be expressed by a high number of PBMCs. This was further corroborated by staining cells with Ab 3, the center-specific antibody, where an extensive shift in fluorescence intensity between negative and positive cells was observed, with the majority of cells staining positive for MAP3K12 (Fig. 6C). Taken together, these data provide evidence of MAP3K12 protein expression in human PBMCs.

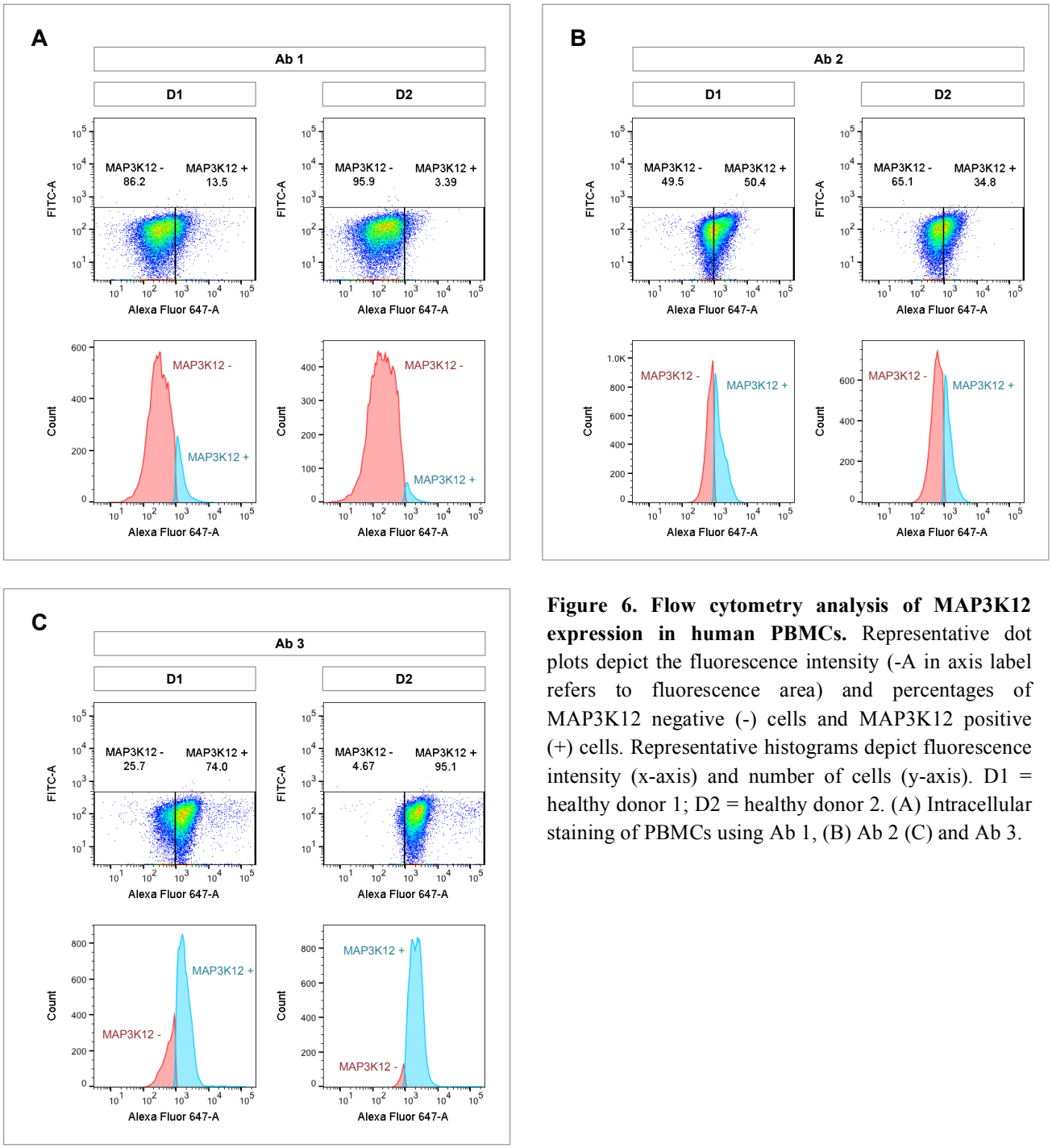


**Figure 6. Flow cytometry analysis of MAP3K12 expression in human PBMCs.** Representative dot plots depict the fluorescence intensity (-A in axis label refers to fluorescence area) and percentages of MAP3K12 negative (-) cells and MAP3K12 positive (+) cells. Representative histograms depict fluorescence intensity (x-axis) and number of cells (y-axis). D1 = healthy donor 1; D2 = healthy donor 2. (A) Intracellular staining of PBMCs using Ab 1, (B) Ab 2 (C) and Ab 3.

# 5 Discussion

Activation of the JNK stress-induced pathway is hypothesized to mediate neurodegeneration observed in ALS[30-32]. MAP3K12 is an essential upstream regulator of this stress-induced apoptotic signaling, and selective small-molecule inhibitors of this kinase have neuroprotective activity *in vitro* and suppression of JNK activation and subsequently downstream responses in injury models[8,12]. Thus, inhibition of MAP3K12 may provide a disease-modifying treatment option for neurodegenerative diseases, such as ALS. Gene expression-based peripheral blood biomarkers would be useful to assess the PD effects of MAP3K12 inhibitors, and for this reason, we asked whether MAP3K12 is expressed on a protein level in blood.

*Map3k12* cKO mouse models are useful negative control for assessing expression of MAP3K12 and its downstream targets in the central nervous system. Here, we demonstrated that *Map3k12* transcript is significantly reduced, not only in brain tissue, but also in peripheral blood from *Map3k12* cKO mice. Remarkably, at the time of gene expression analysis, over a year had elapsed since recombination had been induced through three weeks of tamoxifen treatment in these mice. This implies that this dosing regimen is sufficient to induce a long-lasting reduction in *Map3k12* transcript in both brain and blood in *Map3k12* cKO mice, and thus avoid the lethality observed in embryonic *Map3k12* KO mice. Interestingly, down-regulation of the transcript was observed with probes targeting sequences within the deleted region of the gene, as well as upstream and downstream of it, suggesting that deletion of the exons encoding the kinase domain of MAP3K12 causes the entire transcript to be lost in blood. To summarize, the *Map3k12* cKO mouse model was concluded to be an efficient negative control for assessment of MAP3K12 protein expression in blood as well as for identification of expression-based blood biomarkers following *in vivo* inhibition of MAP3K12.

A crucial step towards identifying potential expression of MAP3K12 in blood was to find specific and sensitive anti-MAP3K12 antibodies. Here, we used western blot to screen a number of antibodies and found three that evidently recognize both human and mouse MAP3K12. Surprisingly, two bands were observed for *Map3k12*$^{loxp}$;Cre$^{neg}$ brain tissue blotted with Ab 2. A possible explanation for this is that the lower molecular weight band could correspond to a splicing variant of MAP3K12 that is only recognized by the N-terminus specific antibody. This in turn suggesting that the splicing event affects the center and C-terminus portion of the protein.

Out of these three antibodies, the antibody targeting a sequence within the central region of MAP3K12 was concluded the most sensitive, hence a promising candidate for exploring MAP3K12 expression in blood using both flow cytometry and western blot. Moreover, it is a potential candidate

for analyzing MAP3K12 using immunohistochemistry, which could enable *in situ* localization of MAP3K12 in different tissues. Establishing the localization and distribution of MAP3K12 in nervous tissue could help us get a better understanding of how it relays stress-induced apoptotic signaling.

Utilizing the three antibodies from the western blot, we developed an intracellular staining method for detection of MAP3K12, which we then used to explore MAP3K12 expression in human PBMCs. These experiments revealed evidence of MAP3K12 expression in human blood. More specifically, MAP3K12 expression was detected with Ab 2 and Ab 3, which recognize the N-terminus and the central region, respectively. As would be expected based on previous protein analyses, flow cytometry analysis using the center-specific antibody (Ab 3) provided the strongest evidence of MAP3K12 expression in blood. Nonetheless, results using two anti-MAP3K12 antibodies of different specificity further support the existence of MAP3K12 protein in blood. However, flow cytometry analysis of MAP3K12 in PBMCs from *Map3k12* cKO mice will help to bolster the evidence of MAP3K12 expression in peripheral blood cells. In addition, it would be of great interest to confirm the expression of MAP3K12 in mouse and human blood by a second, independent method such as western blot. For this purpose, a next step will be to develop an immunoprecipitation method to enrich for MAP3K12 in blood to allow for subsequent detection by western blot.

The heterogeneity of human PBMCs makes it challenging to measure RNA expression, hence identification of specific cell types with relatively high MAP3K12 expression could enable us to narrow down the numbers of genes to study. Remarkably, a great shift in fluorescence intensity was observed for a small fraction of the MAP3K12 positive cells using Ab 3, suggesting that these cells express high levels of the protein. It would be interesting to characterize and identify these cells, since detection of specific cell populations expressing high levels of MAP3K12 could facilitate biomarker detection. Thus, a subsequent effort will be to identify specific cell populations expressing the protein by staining human peripheral blood with a variety of immune cell surface markers concurrently with anti-MAP3K12 antibodies. Additionally, flow cytometry analysis of peripheral blood from *Map3k12* cKO mice would enable us to explore whether any cell populations are especially impacted by the loss of MAP3K12.

In conclusion, we provide evidence of MAP3K12 expression in human peripheral blood, which implies that potential downstream changes in response to MAP3K12 inhibition could be a reflection of target engagement. These findings will allow us to perform RNAseq analysis to identify candidate genes changing in blood in response to MAP3K12 inhibition with the potential to discover expression-based PD blood biomarkers.

# References


1. Przedborski, S., Vila, M. & Jackson-Lewis, V. Series Introduction: Neurodegeneration: What is it and where are we? *Journal of Clinical Investigation* **111,** 3–10 (2003).

2. Taylor, J. P., Brown, R. H. & Cleveland, D. W. Decoding ALS: from genes to mechanism. *Nature* **539,** 197–206 (2016).

3. Weishaupt, J. H., Hyman, T. & Dikic, I. Common Molecular Pathways in Amyotrophic Lateral Sclerosis and Frontotemporal Dementia. *Trends in Molecular Medicine* **22,** 769–783 (2016).

4. Yang, J. *et al.* Pathological axonal death through a MAPK cascade that triggers a local energy deficit. *Cell* **160,** 161–176 (2015).

5. Conforti, L., Gilley, J. & Coleman, M. P. Wallerian degeneration: an emerging axon death pathway linking injury and disease. *Nature Reviews Neuroscience* **15,** 394–409 (2014).

6. Tedeschi, A. & Bradke, F. The DLK signalling pathway--a double-edged sword in neural development and regeneration. *EMBO reports* **14,** 605–614 (2013).

7. Ghosh, A. S. *et al.* DLK induces developmental neuronal degeneration via selective regulation of proapoptotic JNK activity. *The Journal of Cell Biology* **194,** 751–764 (2011).

8. Patel, S. *et al.* Discovery of dual leucine zipper kinase (DLK, MAP3K12) inhibitors with activity in neurodegeneration models. *Journal of Medicinal Chemistry* **58,** 401–418 (2015).

9. Bogoyevitch, M. A. & Arthur, P. G. Inhibitors of c-Jun N-terminal kinases—JuNK no more? *Biochimica et Biophysica Acta (BBA) - Proteins and Proteomics* **1784,** 76–93 (2008).

10. Manning, A. M. & Davis, R. J. Targeting JNK for therapeutic benefit: from junk to gold? *Nature Reviews Drug Discovery* **2,** 554–565 (2003).

11. Cargnello, M. & Roux, P. P. Activation and function of the MAPKs and their substrates, the MAPK-activated protein kinases. *Microbiology and Molecular Biology Reviews* **75,** 50–83 (2011).

12. Welsbie, D. S. *et al.* Enhanced Functional Genomic Screening Identifies Novel Mediators of Dual Leucine Zipper Kinase-Dependent Injury Signaling in Neurons. *Neuron* **94,** 1142–1154 (2017).

13. map3k12. *gtexportal.org* Available at: https://gtexportal.org/home/gene/map3k12. (Accessed: 5 May 2017)

14. Deepak, S.A. *et al.* Real-Time PCR: Revolutionizing Detection and Expression Analysis of Genes. *Current Genomics* **8,** 234–251 (2007).

15. Nijssen, J., Comley, L. H. & Hedlund, E. Motor neuron vulnerability and resistance in amyotrophic lateral sclerosis. *Acta Neuropathologica* **133,** 863–885 (2017).

16. Swinnen, B. & Robberecht, W. The phenotypic variability of amyotrophic lateral sclerosis. *Nature Reviews Neurology* **10,** 661–670 (2014).

17. Schymick, J. C., Talbot, K. & Traynor, B. J. Genetics of sporadic amyotrophic lateral sclerosis. *Human Molecular Genetics* **16,** R233–R242 (2007).

18. Brown, R. H., Jr. Mutations in Cu/Zn superoxide dismutase (SOD1) are associated with familial amyotrophic lateral sclerosis (ALS). *Free Radical Biology and Medicine* **15,** 471 (1993).

19. Peters, O. M., Ghasemi, M. & Brown, R. H., Jr. Emerging mechanisms of molecular pathology in ALS. *Journal of Clinical Investigation* **125,** 1767–1779 (2015).

20. Hosie, K. A., King, A. E., Blizzard, C. A., Vickers, J. C. & Dickson, T. C. Chronic Excitotoxin-Induced Axon Degeneration in a Compartmented Neuronal Culture Model. *ASN Neuro* **4,** AN20110031 (2012).

21. King, A. E. & Vickers, J. C. in *Handbook of Neurotoxicity* 1223–1245 (Springer New York, 2014). doi:10.1007/978-1-4614-5836-4_145

22. Gerdts, J., Summers, D. W., Milbrandt, J. & DiAntonio, A. Axon Self-Destruction: New Links among SARM1, MAPKs, and NAD+ Metabolism. *Neuron* **89,** 449–460 (2016).

23. Widmann, C., Gibson, S., Jarpe, M. B. & Johnson, G. L. Mitogen-activated protein kinase: conservation of a three-kinase module from yeast to human. *Physiological Reviews* **79,** 143–180 (1999).

24. Plotnikov, A., Zehorai, E., Procaccia, S. & Seger, R. The MAPK cascades: Signaling components, nuclear roles and mechanisms of nuclear translocation. *Biochimica et Biophysica Acta (BBA) - Molecular Cell Research* **1813,** 1619–1633 (2011).

25. Hirai, S.I. *et al.* Expression of MUK/DLK/ZPK, an activator of the JNK pathway, in the nervous systems of the developing mouse embryo. *Gene Expression Patterns* **5,** 517–523 (2005).

26. Watkins, T. A. *et al.* DLK initiates a transcriptional program that couples apoptotic and regenerative responses to axonal injury. *Proceedings of the National Academy of Sciences* **110,** 4039–4044 (2013).

27. Pearson, G. Mitogen-Activated Protein (MAP) Kinase Pathways: Regulation and Physiological Functions. *Endocrine Reviews* **22,** 153–183 (2001).

28. Miller, R. G., Mitchell, J. D., Lyon, M. & Moore, D. H. Riluzole for amyotrophic lateral sclerosis (ALS)/motor neuron disease (MND). *Amyotrophic Lateral Sclerosis and Other Motor Neuron Disorders* **4,** 191-206 (2009).

29. The FDA approves Radicava; is it a breakthrough moment for ALS? – DRG Blog – DRG. (2017).

30. Kim, E. K. & Choi, E.J. Pathological roles of MAPK signaling pathways in human diseases. *Biochimica et Biophysica Acta (BBA) - Molecular Basis of Disease* **1802,** 396–405 (2010).

31. Virgo, L. & de Belleroche, J. Induction of the immediate early gene c-jun in human spinal cord in amyotrophic lateral sclerosis with concomitant loss of NMDA receptor NR-1 and glycine transporter mRNA. *Brain Research* **676,** 196–204 (1995).

32. Vlug, A. S. *et al.* ATF3 expression precedes death of spinal motoneurons in amyotrophic lateral sclerosis-SOD1 transgenic mice and correlates with c-Jun phosphorylation, CHOP expression, somato-dendritic ubiquitination and Golgi fragmentation. *European Journal of Neuroscience* **22,** 1881–1894 (2005).

33. Pozniak, C. D. *et al.* Dual leucine zipper kinase is required for excitotoxicity-induced neuronal degeneration. *Journal of Experimental Medicine* **210,** 2553–2567 (2013).

34. Borsello, T. *et al.* A peptide inhibitor of c-Jun N-terminal kinase protects against excitotoxicity and cerebral ischemia. *Nature Medicine* **9,** 1180–1186 (2003).

35. Kim, B.J. *et al.* In vitro and in vivo neuroprotective effects of cJun N-terminal kinase inhibitors on retinal ganglion cells. *Molecular Neurodegeneration* **11,** 30 (2016).

36. Welsbie, D. S. *et al.* Functional genomic screening identifies dual leucine zipper kinase as a key mediator of retinal ganglion cell death. *Proceedings of the National Academy of Sciences of the United States of America* **110,** 4045–4050 (2013).

37. Zhao, X., Modur, V., Carayannopoulos, L. N. & Laterza, O. F. Biomarkers in Pharmaceutical Research. *Clinical Chemistry* **61,** 1343–1353 (2015).

38. Bakkar, N., Boehringer, A. & Bowser, R. Use of biomarkers in ALS drug development and clinical trials. *Brain Research* **1607,** 94–107 (2015).

39. Turner, M. R., Kiernan, M. C., Leigh, P. N. & Talbot, K. Biomarkers in amyotrophic lateral sclerosis. *The Lancet Neurology* **8,** 94–109 (2009).

40. Kondoh, K. & Nishida, E. Regulation of MAP kinases by MAP kinase phosphatases. *Biochimica et Biophysica Acta (BBA) - Molecular Cell Research* **1773,** 1227-1237 (2007).

41. Hayashi, S. & McMahon, A. P. Efficient Recombination in Diverse Tissues by a Tamoxifen-Inducible Form of Cre: A Tool for Temporally Regulated Gene Activation/Inactivation in the Mouse. *Developmental Biology* **244,** 305–318 (2002).

42. Huntwork-Rodriguez, S. *et al.* JNK-mediated phosphorylation of DLK suppresses its ubiquitination to promote neuronal apoptosis. *The Journal of Cell Biology* **202,** 747–763 (2013).

43. Krutzik, P. O. & Nolan, G. P. Intracellular phospho-protein staining techniques for flow cytometry: Monitoring single cell signaling events. *Cytometry* **55A,** 61–70 (2003).

44. Seita, J. & Weissman, I. L. Hematopoietic stem cell: self-renewal versus differentiation. *Wiley Interdisciplinary Reviews: Systems Biology and Medicine* **2,** 640–653 (2010).

# Supplemental Information

**Table S1.** Primary and secondary antibodies used in this study. Abbreviations: Rabbit (Rb), Mouse (Ms), Human (Hu), Rat (Rt), Non-human primate (Nhp), Bovine (Bv), Pig (Po), Do (Donkey), mAb (monoclonal antibody) and pAb (polyclonal antibody).

| # | Antibody | Target | Description | Species reactivity | Supplier |
|---|---|---|---|---|---|
| 1 | Anti-MAP3K12 | C-terminus of MAP3K12 | Rb mAb | Ms, Hu | Genentech |
| 2 | Anti-MAP3K12 | N-terminus of MAP3K12 | Rb mAb | Ms, Hu | Genentech |
| 3 | Anti-MAP3K12 | Center region of MAP3K12 | Rb pAb | Ms, Hu | Sigma Aldrich (#SAB2700169) |
| 4 | Anti-MAP3K12 | C-terminus of MAP3K12 | Rb pAb | Ms, Hu | Abcam (# ab37996) |
| 5 | Anti-MAP3K12 | Center region of MAP3K12 | Rb pAb | Ms, Rt, Hu | Novus Biologicals (#NBP1-46063) |
| 6 | Anti-MAP3K12 | MAP3K12 (region N/A) | Rb pAb | Ms, Rt, Hu | Biorbyt (# orb335162) |
| 7 | Anti-MAP3K12 | MAP3K12 (region N/A) | Ms mAb | Ms, Hu | Sigma Aldrich (#SAB1306766) |
| 8 | β-Actin (13E5) | Endogenous levels of total β-actin protein | Rb mAb (HRP conjugate) | Hu, Ms, Rt, Nhp, Bv, Po | Cell signalling technology (#5125S) |
| 9 | Alexa Fluor 647 | Heavy and light chains of Rb IgG | Do pAb (conjugated with Alexa Fluor® 647) | Rb | Biolegend (#406414) |
| 10 | Rabbit IgG isotype control | Control for Rb IgG antibodies | Rb | Rt | Thermo Fischer Scientific (#02-6102) |
| 11 | Gt anti-Rb IgG Secondary | Heavy and light chains of Rb IgG | Gt pAb | Rb | Thermo Fischer Scientific (#31460) |

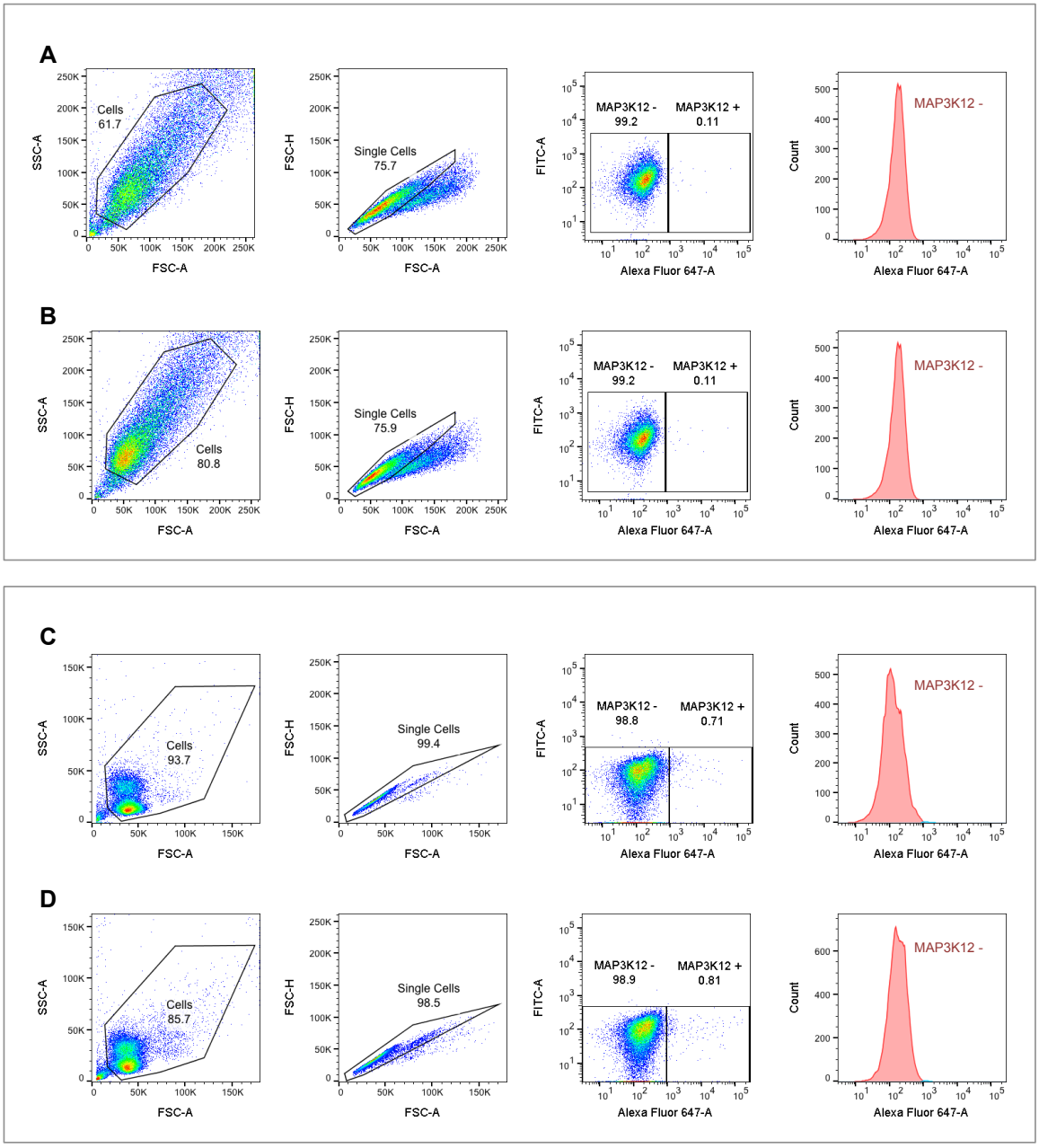


**Figure S1. Gating strategy for flow cytometry analysis.** Cells were selected based on FSC-area (FSC-A) and SSC-area (SSC-A). Single cells were separated from doublets based on FSC-A and FSC-height (FSC-H). Fluorescence-detecting gates (dot plots and histograms) were set in accordance to cells stained positive with IgG isotype control (MAP3K12 -) and a secondary antibody fluorescence dye Alexa Fluor 647 (-A in axis label refers fluorescence area). (A) Non-induced 293 cells. (B) DOX-induced 293 cells. (C) Human PBMCs from healthy donor 1 (D) and healthy donor 2.